Tetrahedron 162 (2024) 134115

Contents lists available at ScienceDirect

Tetrahedron

journal homepage: www.elsevier.com/locate/tet

Isolation of Caribbean Ciguatoxin-5 (C-CTX5) and confirmation of its structure by NMR spectroscopy

Christopher O. Miles [a,b], Ian W. Burton [c], Nancy I. Lewis [a], Alison Robertson [d,e], Sabrina D. Giddings [a], Pearse McCarron [a], Elizabeth M. Mudge [a,*]

[a] Biotoxin Metrology, National Research Council, 1411 Oxford Street, Halifax, NS, B3H 3Z1, Canada
[b] Norwegian Veterinary Institute, P.O. Box 64, 1431, Ås, Norway
[c] Aquatic and Crop Resources Development Research Center, National Research Council, 1411 Oxford Street, Halifax, NS, B3H 3Z1, Canada
[d] Stokes School of Marine & Environmental Sciences, University of South Alabama, 600 Clinic Drive, Mobile, AL, 36688, USA
[e] Marine Ecotoxicology Group, Dauphin Island Sea Lab, 101 Bienville Blvd, Dauphin Island, AL, 36528, USA

ARTICLE INFO

Keywords:
Ciguatera
Structure confirmation
NMR
LC−HRMS
Caribbean ciguatoxin

ABSTRACT

Ciguatera poisoning occurs throughout subtropical and tropical regions globally. The Virgin Islands in the Caribbean Sea is a known hyperendemic region for ciguatera and has been associated with Caribbean ciguatoxin (C-CTX) contamination in fish. An algal C-CTX (C-CTX5) was identified in *Gambierdiscus silvae* and *G. caribeaus* isolated from benthic algal samples collected in waters south of St. Thomas, US Virgin Islands. The highest CTX-producing isolate, *G. silvae* 1602 SH-6, was grown at large-scale to isolate sufficient C-CTX5 for structural confirmation by NMR spectroscopy. A series of orthogonal extraction and fractionation procedures resulted in purification of approximately 40 μg of C-CTX5, as estimated by quantitative NMR. A suite of 1D and 2D NMR experiments were acquired that verified the structure originally proposed for C-CTX5. The structural confirmation and successful isolation of C-CTX5 opens the way for work on the stability, toxicology and biotransformation of C-CTXs, as well as for the production of quantitative reference materials for analytical method development and validation. The strategies developed for purification of C-CTX5 may also apply to isolation and purification of CTXs from the Pacific Ocean and other regions.

1. Introduction

Ciguatera poisoning (CP) is caused by the consumption of fish or other marine seafood contaminated with ciguatoxins (CTXs). CP can appear as a myriad of symptoms ranging from gastrointestinal, neurological and cardiovascular, with symptoms lasting from days to months. There is a wide spectrum of symptoms and severity, making it a complex seafood illness. CP has been described as a neglected disease due to its sporadic occurrence and high prevalence in tropical and subtropical regions [1]. There are an estimated 10,000 to 50,000 cases annually [2] and CP is rapidly becoming a global concern due to changes in reef ecosystems, ocean temperatures, increased travel, and international trade in fish.

Ciguatoxins (CTXs) are a class of neutral polyethers confirmed to be produced by *Gambierdiscus* spp. [3–5]. They are historically classified based on regional variations in CTX profiles observed in fish, but have recently been re-classified based on backbone structures into four groups including CTX1B, CTX3C and Caribbean CTXs (C-CTXs) [1]. To date, the structure of the fourth group, CTXs from the Indian Ocean, remains undescribed. CTX1B and CTX3C have historically been detected in fish and microalgae from the Pacific Ocean, while C-CTXs were originally detected in fish harvested in the Caribbean Sea [6] and are also implicated in CP events in the eastern Atlantic Ocean [7]. Ciguatoxins are consumed by marine organisms grazing on macroalgae, seagrass, and other benthic substrates where *Gambierdiscus* spp. are attached, and the toxins are subsequently bioaccumulated and biotransformed in higher trophic levels species [8,9]. A variety of reef fish have been linked to CP including barracudas, snappers, groupers, and amberjacks, as well as lower trophic-level fish (parrotfish) and reef invertebrates [1].

Caribbean ciguatoxin-1 (C-CTX1) was first isolated from fish harvested in the Caribbean region and its structure elucidated in 1998 by mass spectrometry and NMR spectroscopy [6]. The polyether backbone is composed of 14 fused polyether rings (A–N) with a C-3 hydroxy group and an N-ring hemiketal at C-56 (Fig. 1). Recently, additional

* Corresponding author.
E-mail address: Elizabeth.mudge@nrc-cnrc.gc.ca (E.M. Mudge).

https://doi.org/10.1016/j.tet.2024.134115
Received 19 April 2024; Received in revised form 13 June 2024; Accepted 17 June 2024
Available online 18 June 2024

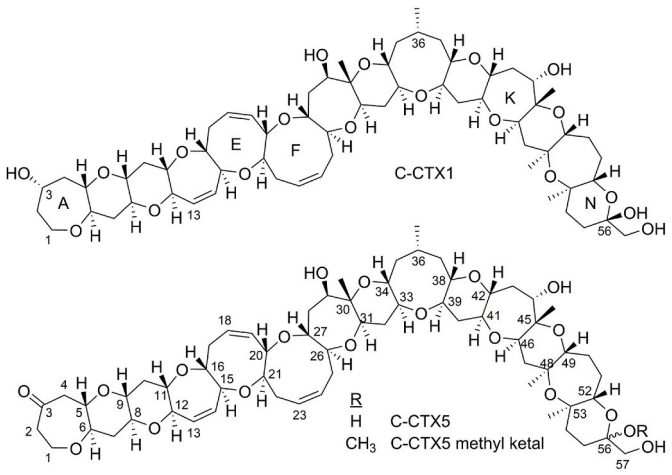

Fig. 1. Structures of C-CTX1 [6] and of C-CTX5 as proposed by Mudge et al. [3], as well as of the 56-methyl ketal derivative of C-CTX5 used during purification of C-CTX5.

fish-derived C-CTXs, C-CTX3 and C-CTX4, have been structurally characterized as the ring-N-*seco* forms reduced at C-56, through a series of chemical reactions including borohydride reduction and periodate cleavage in combination with LC−HRMS analysis [10]. A similar approach was then applied to the identification of C-CTX5, the first C-CTX reported to be produced by an alga, in *Gambierdiscus silvae* and *G. caribeaus* isolates collected from reefs surrounding waters near St. Thomas, US Virgin Islands [3]. The structure of C-CTX5 was proposed to contain a C-3 ketone, which upon reduction yields C-CTX1, the dominant C-CTX reported in fish associated with CP in the Caribbean Sea.

The aim of this work was to bulk culture the C-CTX5-producing strain, *G. silvae* 1602 SH-6, in order to isolate sufficient quantities for structural confirmation by NMR spectroscopy. Isolation was achieved by developing a series of novel purification steps to isolate C-CTX5. A series of 1-D and 2-D NMR spectra, including HSQC and HMBC data acquired using non-uniform sampling (NUS), were obtained to confirm the originally-proposed structure of C-CTX5.

2. Methods

2.1. Reagents

MeOH, MeCN and formic acid (~98 %) were LC–MS grade from ThermoFisher Scientific (Ottawa, ON, Canada; Waltham, MA, USA). Dichloromethane was from Caledon Laboratories (Georgetown, ON, Canada). Methyl *tert*-butyl ether (MTBE; HPLC grade), tetrahydrofuran (THF; 99.9 %), trifluoroacetic acid (99.0 %), diethylamine (99.5 %), potassium carbonate and boric acid gel were from Millipore–Sigma (Oakville, ON, Canada). Distilled water was ultra-purified to 18.2 MΩ × cm using a Milli-Q purification system (Millipore–Sigma). Pyridine-d_5 (D, 99.94 %) was from Cambridge Isotope Laboratories (Tewksbury, MA, USA).

2.2. Culturing & harvesting

Gambierdiscus silvae (1602 SH-6) was established in culture following isolation from *Dictyota* spp., collected from Seahorse Shoal, St. Thomas, U. S. Virgin Islands as described by Mudge et al. [3]. The culture was grown in 1 L batches on L1(−Si) medium [11], supplemented with 0.05 mM NH_4Cl, in 2.8 L Fernbach flasks. Cultures were incubated at 25 °C under a 12:12 L:D photoperiod with a photon flux of 55–65 μmol m^{-2} s^{-1} cool white light. When cell density reached 4–5 × 10^3 cells L^{-1}, cultures were concentrated using a 20 μm Nitex net. Cells that had adhered to the bottom of the flask were gently removed using a rubber spatula and added to a small volume of the filtrate (~500 mL). The cell concentrates were stored at −20 °C until processing. Due to the potential risks associated with the toxic microalgae, masks and suitable personal protective equipment were worn during handling and harvest of the culture.

2.3. Isolation procedure

G. silvae concentrates were processed in 1 L batches equating to approximately 20–30 L of harvested culture per batch. The concentrates underwent three freeze–thaw cycles by thawing the contents at ambient temperature and freezing at −20 °C overnight in order to release the CTXs into the medium. Cellular debris was removed by vacuum filtration with a Büchner funnel fitted with a Whatman GF/C filter, and the filtrate (~1 L) was transferred to a 2 L separatory funnel and extracted with methyl *tert*-butyl ether (MTBE; 5 × 200 mL). Residual water was removed from the combined ethereal fractions with Na_2SO_4. The MTBE fractions were pooled, evaporated under vacuum at 40 °C, and the residue was dissolved in MeCN containing 1 % diethylamine (25 mL). Pre-prepared boric acid gel (1 g) [12] and ~20 3 Å molecular sieves were added, the solution was placed on a Thermolyne Maxi-Mix III shaker (Thermo Scientific) at 200 rpm for 2 h at ambient temperature, and the solvent was removed from the gel with a pipette and the gel washed with MeCN containing 1 % diethylamine (5 mL). CTXs bound to the gel were extracted with 9:1 THF–H_2O containing 1 % formic acid (25 mL), by shaking (2 h, 200 rpm). Solvent was removed with a pipette, and the gel was extracted a second time overnight (~16 h) with a fresh aliquot of 9:1 THF–H_2O containing 1 % formic acid (25 mL) using gentle shaking. The extracts were pooled and filtered through a Whatman no. 1 filter paper. Residual acid was neutralized with aqueous K_2CO_3 (2 g/mL; 1 mL) and the solvent was evaporated under vacuum at 40 °C. The CTX-containing residue was dissolved in CH_2Cl_2 (500 μL) and fractionated using flash chromatography on a silica gel cartridge (4 g, RediSep Silica, 20–40 μm; Teledyne ISCO, NE, USA). The cartridge was equilibrated with CH_2Cl_2 and operated with a flow rate of 12 mL/min. The sample was loaded and subjected to the following linear gradient: 0–1 min: 100 % CH_2Cl_2; 1–25 min: 0–10 % MeOH in CH_2Cl_2; 25–26 min: 10–100 % MeOH in CH_2Cl_2; 26–30 min: 100 % MeOH. Fractions were collected in 0.75 min increments. Fraction 12 (9 min) contained C-CTX5 and was evaporated to dryness under N_2 at 40 °C. The residue was dissolved in MeOH (500 μL), trifluoroacetic acid (50 μL) was added, the sample was mixed by vortex, and allowed to stand at ambient temperature for 2 h. The resulting solution of C-CTX5 56-methyl ketal was neutralized with aqueous 10 % K_2CO_3 (5 mL) and extracted with MTBE (5 × 3 mL). The organic layers were combined, evaporated to dryness under N_2, and dissolved in 50 % MeCN (200 μL). C-CTX5 56-methyl ketal was isolated using an Agilent 1100 semi-preparative HPLC comprised of a quaternary pump, temperature controlled autosampler, column compartment and fraction collector and coupled to a UV detector monitoring at 210 nm. Purification was achieved using a Luna C18(2) column (250 × 10 mm, 3 μm; Phenomenex, Torrance, CA, USA) eluted isocratically with 80 % MeCN at 2 mL/min for 30 min, with 25 μL injections, and 1.0 mL fractions were collected between 24 and 28 min. The column was washed with 100 % MeCN for approximately 10 min following each run, and re-equilibrated with 80 % MeCN. Fractions containing C-CTX5 56-methyl ketal were confirmed by LC−HRMS, pooled in a round-bottomed flask, and the organic solvent was removed under vacuum at 40 °C. The aqueous residue was transferred to an 8 mL glass tube, and the round-bottomed flask was rinsed with an approx. equal volume of MeCN, which was added to the glass tube. The methyl ketal was hydrolyzed to C-CTX5 by addition of trifluoroacetic acid (200 μL) and allowing the solution to react at ambient temperature for 2 h. Residual acid was removed by applying the solution (~1:1 MeCN–water) to a preconditioned (MeCN, then H_2O) solid phase extraction (SPE) cartridge Strata-X RP 200 mg (Phenomenex), washing the SPE cartridge with H_2O (3 mL), and then with 50 % MeCN (3 mL). The

C-CTX5 was eluted with 70 % MeCN (6 mL), the MeCN evaporated under N_2, and the resulting aqueous fraction was extracted with MTBE (3 × 3 mL). The MTBE extract was evaporated to dryness under N_2 to give pure C-CTX5 as a colourless solid, which was dissolved in MeOH (500 μL), and stored at −20 °C until required.

2.4. LC–HRMS analysis

Analyses were performed using an Agilent 1290 Infinity II LC equipped with a binary pump, autosampler (10 °C) and column compartment (40 °C) (Agilent Technologies, Mississauga, ON, Canada) coupled to a Q Exactive HF Orbitrap mass spectrometer (Thermo Fischer Scientific, Waltham, MA, USA) with a heated electrospray ionization probe (HESI-II). Chromatographic separation used a Kinetex F5 UHPLC column (100 × 2.1 mm, 1.7 μm; Phenomenex) with gradient elution and mobile phases composed of 0.1 % formic acid in H_2O (A) and 0.1 % formic acid in MeCN (B). The injection volume was 5 μL and gradient (0.3 mL/min) was: 0–18 min, 30–60 % B; 18–18.1 min, 60–99 % B; 18.1–22 min, 99 % B; followed by an 8 min re-equilibration at 30 % B [3].

Full-scan acquisition was performed with positive ionization over a mass range of *m/z* 1000–1250. The spray voltage of the source was +4.5 kV, with a capillary temperature of 340 °C. The sheath and auxiliary gas were set at 40 and 10 (arbitrary units), respectively. The probe heater temperature was set at 150 °C and the S-Lens RF level was set to 100. The mass resolution setting was 120,000 with an automatic gain control target of 1×10^6 and a maximum injection time of 100 ms per scan.

2.5. NMR spectroscopy

The C-CTX5 was transferred to a high-recovery vial, and the storage vessel was rinsed with pyridine-d_5 to ensure complete recovery. The solution was evaporated to dryness under a stream of nitrogen at ambient temperature. Under a curtain of argon, the residue was dissolved in 200 μL of pyridine-d_5, and evaporated under a stream of nitrogen as above. The evaporation and reconstitution steps were repeated three times to ensure removal of residual non-deuterated solvent and water. Using a dry gas-tight syringe under a curtain of argon, 630 μL of pyridine-d_5 was added to the high-recovery vial, which was gently vortex-mixed and allowed to stand for 1.5 h to ensure the sample was completely dissolved. The dried gas tight syringe was then used to transfer 600 μL of the C-CTX5 solution to a prerinsed and dried 5 mm NMR tube (Wilmad, Vineland, NJ, USA) for the 1-D and 2-D NMR spectra acquisition. The sample was subsequently removed from the 5 mm NMR tube, evaporated to dryness under N_2, dissolved in 30 μL pyridine-d_5 and transferred to a 1.7 mm NMR tube (Bruker Ltd., Milton, ON, Canada) for acquisition of an HMBC NMR spectrum using a microprobe.

NMR spectra were acquired on a Bruker Avance III 700 NMR spectrometer (Bruker Ltd., Milton, ON, Canada) running at 700.08 MHz for ^{1}H and 176.035 MHz for ^{13}C. In order to estimate the quantity of C-CTX5, a quantitative ^{1}H NMR spectrum was acquired using a calibrated 90° pulse and an interpulse delay of 15 s and quantified against an external standard of 4.09 mM caffeine (USP grade, Sigma, Oakville ON) gravimetrically determined in D_2O in a flame-sealed high-precision NMR tube (Wilmad) using the protocol previously described by Burton et al. [13]. The resonance at 3.85 ppm (H-1α) was used for quantitation of C-CTX5.

In order to confirm the structure, a suite of 1-D and 2-D NMR spectra were acquired: DQF-COSY; TOCSY (120 ms mixing time); NOESY (300 ms mixing time); ^{1}H–^{13}C multiplicity-edited HSQC; ^{1}H–^{13}C HMBC (60 ms mixing time); ^{13}C and ^{1}H NMR spectra. There was a significant water resonance at approximately 5.0 ppm in the initial ^{1}H NMR spectrum, so the ^{1}H NMR spectrum was acquired with suppression of the water resonance at 4.997 ppm using on-resonance presaturation. Due to the low amount of compound (42 μg as determined by qNMR), the ^{13}C NMR spectrum showed few resonances. Therefore, the reported ^{13}C chemical shifts were determined from the HSQC and HMBC spectra. In addition, to improve the resolution in the F1 dimension of the HSQC spectrum, a non-edited HSQC NMR spectrum was acquired using NUS and 4096 points acquired in T1, with an NUS sampling sparsity of 5 % and 1024 scans per increment for a total acquisition time of 49 h 37 min. This was done primarily to resolve the methylene carbons between 37 and 38 ppm. An HMBC spectrum was also run using NUS, with 300 points acquired in T1 and an NUS sampling sparsity of 25 %. After transfer of the sample to a 1.7 mm NMR tube, a second HMBC spectrum was obtained with a microprobe with 1024 points acquired in T1 and an NUS sparsity of 12 % and 2048 scans per increment for a total acquisition time of 81 h 12 min. Spectra were processed using TopSpin v 3.6.5 or 4.2.0 (Bruker Ltd., Milton, ON, Canada). All spectra were referenced to the highest-field resonance of the residual protonated pyridine-d_5 solvent in the 1-D spectra at 7.21 ppm (^{1}H) and 123.5 ppm (^{13}C) to facilitate direct comparison with the assignments of Lewis et al. [6] for C-CTX1. The spectrometer reference frequencies from the 1-D spectra were then used to reference the 2-D spectra.

3. Results & discussion

3.1. Culturing of G. silvae 1602 SH-6

The microalgal culture, originally supplied in K medium at a salinity of 35 ‰, was transferred and acclimated to L1(−Si) medium at a salinity of 32 ‰. Analysis of cell counts and toxin production indicated minimal impact on cell growth or toxin production under the adjusted conditions. Fernbach flasks containing approximately 1 L of culture were grown to cell counts of approximately 4×10^3 cells/mL at time of harvest (day 25–30). A total of approximately 200 L of *G. silvae* 1602 SH-6 was harvested in batches of 20–30 L.

3.2. Isolation protocol

Three 1-L cultures were initially used to assess the extraction of C-CTX5 from the cells, with the goal of reducing matrix components that might interfere with downstream isolation. For this, the cells in medium were exposed a minimum of three freeze–thaw cycles with the intention of releasing the C-CTX5 from the cells into the medium. The medium was filtered and the filtrate was partitioned with an ether-based solvent, as previously used for partitioning neutral CTXs [14,15]. These experiments confirmed that diethyl ether and MTBE could be used interchangeably, as C-CTX5 present in the medium was readily partitioned into both solvents. Extraction of the aqueous filtrate (rather than the biomass) with ethers was performed in order to extract neutral water-soluble organic compounds while excluding highly polar and charged organic compounds, and cellular components (such as pigments), that have the potential to complicate subsequent purification steps. In order to assess the extraction efficiency, C-CTX5 was measured in the ethereal fraction (73–83 %), the resulting cellular material remaining on the filter (14–24 %), and in the spent medium after concentration on a C18 SPE cartridge (2–3%) (Fig. 2). The resulting orange ethereal fraction was a concentrated extract of C-CTXs suitable for further isolation, while the majority of the other cellular components remained in the cells (Fig. S1).

Subsequent isolation steps were performed on batches of approximately 20–30 L culture-equivalents that were concentrated to 1-L during harvesting. The focus of this isolation protocol was on production of highly purified C-CTX5, rather than on yield, and therefore further optimization of the procedure is anticipated for production of larger quantities of C-CTX5.

The colour of the ethereal C-CTX extract obtained from partitioning of the filtered medium was indicative of the presence of pigments (e.g. carotenoids). This solution was evaporated under vacuum and the resulting residue was dissolved in MeCN with 1 % diethylamine for

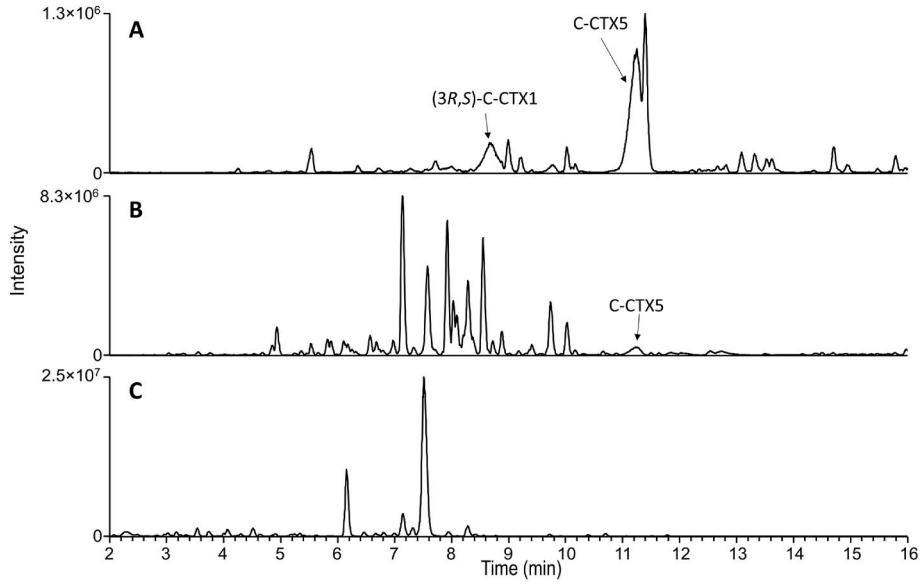

Fig. 2. LC–HRMS total-ion chromatogram (TIC) of a 1-L trial for C-CTX5 extraction showing: (A) MTBE extract of the filtered medium; (B) the extract from the cellular material on the filter, and; (C) the SPE C18 extract of the medium after the MTBE extraction.

adsorption onto boric acid gel [12]. The protocol, which selectively extracts compounds containing 1,2-diols such as C-CTXs, was scaled relative to the peak area of C-CTX5 in each batch of extract. The majority of the pigments remained in the MeCN following the addition of the gel. After removal of the solvent and a washing step, C-CTXs were eluted from the gel with THF–H_2O containing 1 % formic acid resulting in a nearly colourless extract. The acid was neutralized with potassium carbonate prior to solvent removal. The residue was dissolved in dichloromethane, subjected to normal-phase flash chromatography on silica gel, and the C-CTX5-containing fractions were pooled and evaporated to dryness under a stream of N_2.

Preliminary investigations indicated considerable losses of C-CTX5 during semi-preparative reversed-phase HPLC due to significant peak broadening, a characteristic attributable to on-column epimerization at C-56 in the case of C-CTX1 [10]. Attempts with non-acidified mobile phase did not significantly improve this behaviour. Additionally, due to their similar retention times and the peak broadening behaviour, overlap of the C-CTX1 peak with C-CTX5 was observed for fractions containing higher proportions of C-CTX1. Derivatization of C-CTX1 as its 56-ketals was reported to result in much better peak shapes during LC-MS analysis [16]. Therefore, reaction with MeOH containing trifluoroacetic acid [16,17] was used to convert C-CTX5 to its 56-methyl ketal, and the reaction mixture was neutralized with potassium carbonate. The resulting C-CTX5 56-methyl ketal, which exhibited improved peak shape on reverse-phase LC, was purified by semi-preparative reverse-phase HPLC using a non-acidified mobile phase in order to inhibit any on-column hydrolysis to C-CTX5. Fractions containing C-CTX5 56-methyl ketal were pooled and the ketal was hydrolyzed back to C-CTX5.

The final step in the purification involved application of the

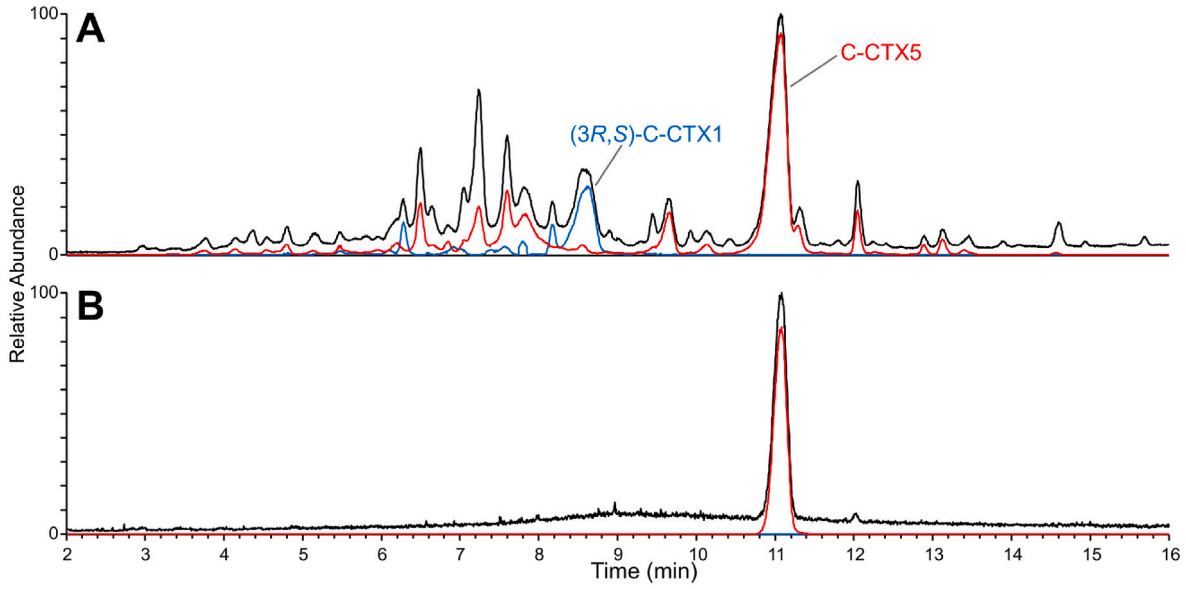

Fig. 3. LC–HRMS TIC (black lines, mass range: *m/z* 1000–1250) of: (A) the MTBE extract of the *G. silvae* 1602 SH-6 filtrate, and; (B) purified C-CTX5 following the isolation procedure. The red and blue lines are summed intensities of all isotopologue peaks exceeding 1 % intensity relative to the monoisotopic $[M + H]^+$ ion at the *m/z* values (±5 ppm) of $[M + H - 2H_2O]^+$, $[M + H - H_2O]^+$, $[M + H]^+$, $[M + NH_4]^+$, and $[M + Na]^+$ for C-CTX5 and C-CTX1, respectively.

hydrolyzed extract to a reverse-phase SPE cartridge, and elution with a stepwise gradient to separate the C-CTX5 from residual acid and any non-hydrolysable contaminants that might have coeluted with the ketal during semi-preparative HPLC. Due to the low quantity (~40 μg), the absolute purity and recovery of C-CTX5 could not be determined, but LC−HRMS analysis (Fig. 3) showed that it was free of other CTX analogues and other major contaminants. Any contaminants originating from the alga in the purified C-CTX5 must be medium-polarity (i.e. extractable with water) neutral organic compounds (i.e. partition into ethers) that contain a boronic-acid-reactive 1,2- or 1,3-diol (i.e. binding to boric acid gel) with similar retention on silica gel to C-CTX5. Furthermore, such contaminants must also reversibly form derivatives with acidic methanol that have similar retention to C-CTX-5 56-methyl ketal on reverse-phase HPLC, and have similar chromatographic retention to C-CTX5 on a reverse-phase SPE after deprotection. The high purity of such a small sample of C-CTX5 is therefore attributable to the selectivity and orthogonality of the steps used in its purification.

3.3. Structure confirmation of C-CTX5 by NMR spectroscopy

The previous work using LC–HRMS/MS together with isotopic exchange reactions, as well as chemical reactions and in vitro biotransformations to known compounds, established that C-CTX5 was the 3-oxo-derivative of the 3-hydoxylated ciguatoxin C-CTX1 [3]. The structure of C-CTX1 was originally established by mass spectrometry and an extensive series of 1-D and 2-D NMR spectroscopy experiments [6], with the absolute stereochemistry assumed to be shared with that previously established for CTX3C [5], with which C-CTX1 shares many structural similarities. However, confirmation of the structure of C-CTX5 by NMR spectroscopy is desirable in order to verify the structural relationship between C-CTX1 and C-CTX5, and with the Pacific CTXs. A series of 1-D and 2-D NMR spectra were therefore obtained from the purified C-CTX5 using d_5-pyridine as solvent (Figs. S2–S19) to allow direct comparison of its chemical shifts with those reported for C-CTX1 [6].

The backbone structure of C-CTX5 was established using COSY and TOCSY NMR experiments (Figs. S5 and S6), which identified a series of ^{1}H–^{1}H spin systems from H-1 to H-2, H-4 to H-29, H-31 to H-44, H-46 to H-47, H-49 to H-52, H-54 to H-55, and H-57 (Fig. 4 and Fig. S20). Four singlet methyl groups and one doublet methyl group were identified in the ^{1}H and HSQC NMR spectra (Figs. S2 and S4, S7–S14), which not only provided the ^{13}C NMR chemical shifts for all protonated carbon atoms in C-CTX5, but also revealed the presence of an oxygenated methylene group (3.96 ppm) that was weakly spin-coupled to a hydroxy group at 6.57 ppm. This showed a correlation in the TOCSY spectrum (Fig. S6) and COSY spectrum (Fig. S5) and can be ascribed to the hydroxymethyl group (C-57) attached to the hemiketal at C-56. An HMBC NMR spectrum was obtained using NUS (Fig. S15) that had relatively low signal-to-noise due to the small amount of C-CTX5 available, but was nonetheless able to confirm the locations of the methyl groups, and to provide the ^{13}C chemical shifts of the quaternary carbons that were not available in the original study of C-CTX1. An additional HMBC NMR spectrum obtained with a microprobe using NUS (Figs. S16–S18) gave better signal-to-noise, providing additional correlations as well as confirming those obtained using the 5 mm probe. Although the signal-to-noise ratio in the NOESY spectrum (Fig. S19) was also limited, sufficient correlations were observed to confirm the positions and orientations of most of the ring-bridging protons, as well as the preferred conformation in the A-ring of C-CTX5 (Fig. 5 and Fig. S20). Correlations observed in the HMBC and NOESY spectra (e.g. Figs. 4 and 5) were sufficient to identify the connections between all of the spin systems.

While the assignments (Table 1) obtained from the NMR spectra of C-CTX5 were mostly identical to those reported by Lewis et al. [6] for C-CTX1 in d_5-pyridine (Figs. 6 and 7, S21 and S22), major differences were observed for many of the resonances arising from the A-ring. In particular, the ^{1}H–^{1}H-coupled spin system that in C-CTX1 continues

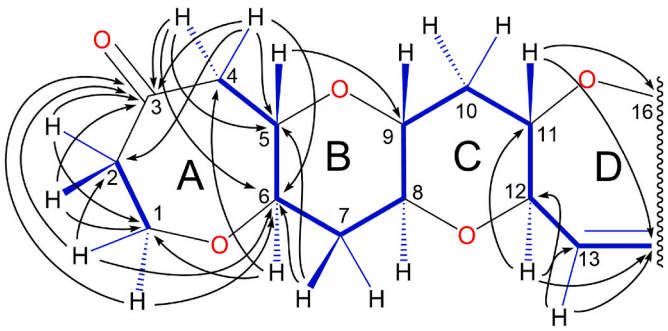

Fig. 4. ^{1}H–^{1}H-coupled spin systems (blue) identified from COSY and TOCSY NMR spectra in the ring-A–D region of C-CTX5, and the observed HMBC correlations.

from H-1 to H-29, was interrupted at C-3 in C-CTX5, consistent with the presence of a non-protonated carbon at C-3. Direct comparison of the published COSY and HSQC spectra of C-CTX1 [6] with those for C-CTX5 (Fig. 7 and S22) showed a marked displacement of ^{1}H and ^{13}C resonances associated with C-1, C-2 and C-4 to C-6, with no resonances attributable to C-3 or H-3 in the COSY, TOCSY, NOESY or HSQC spectra of C-CTX5. However, in the HMBC spectrum of C-CTX5, both of the H-2 resonances showed correlations to C-1 and to a quaternary carbon at 207.5 ppm (Figs. 4 and 5, and S15–S17). Similarly, both H-4 resonances showed HMBC correlations to C-5 and C-6, and to the carbon at 207.5 ppm (Figs. 4 and 5, and S15–S17). Both sets of HMBC correlations are consistent with the presence of a ketone at C-3 of C-CTX5. The NMR data obtained for C-CTX5 thus confirms its structure as 3-oxoC-CTX1, as originally established by Mudge et al. [3] using chemical derivatization and mass spectrometric methods. These data also provides further confirmation of the structure of C-CTX1 established by Lewis et al. [6], and the C-CTX3/4 complex [10,18], because Mudge et al. [3] demonstrated reduction of C-CTX5 to both sets of compounds during their original studies establishing the structure of C-CTX5. Furthermore, Mudge et al. [18] subsequently showed that chemical and biochemical reduction of C-CTX5 resulted in epimeric pairs of the 3-hydroxylated derivatives C-CTX3/4, and that C-CTX1 and C-CTX3/4 were present as epimeric pairs in naturally contaminated fish. The results obtained by Mudge et al. [3]; (2024) are therefore consistent with the primary precursor to the C-CTXs found in fish being the 3-oxo-variant, C-CTX5.

Direct analysis of purified C-CTX5 by NMR spectroscopy unambiguously confirms it to be the 3-oxo-derivative of C-CTX1, as originally proposed by Mudge et al. [3]. Additionally, the close similarity of the ^{1}H and ^{13}C chemical shifts, and the detected ^{1}H multiplicities and NOESY correlations, are consistent with C-CTX1 and C-CTX5 as having the same stereochemistry at all common chiral centres. The identification of the 3-keto-containing C-CTX5 in *G. silvae* and *G. caribaeus* as a major precursor of the known C-CTXs [3] is consistent with the observed presence of mixtures of 3*R*- and 3*S*–C-CTX1, -C-CTX3 and -C-CTX4 in naturally contaminated fish and in aging *G. silvae* cultures [18].

Estevez et al. [19] recently proposed a structural revision of the N-ring of C-CTX1 to a 7-membered ring containing a 56,57-diol closed with a hemiacetal linkage between C-52 and C-57, based on unit-resolution LC–MS/MS data [19]. However, in the present study the edited HSQC NMR spectrum of the C-CTX1 precursor, C-CTX5, showed that C-57 was a hydroxymethyl group, a result consistent with the observed products from periodate cleavage of C-CTX1 [10]. Furthermore, the H-54a, H-55a, H-55b, and H57a,b methylene resonances of C-CTX5 all showed ^2J or ^3J HMBC correlations to the C-56 hemiketal at 96.3 ppm (Fig. S18). Additionally, Sasaki et al. [20] synthesized the J–N rings of C-CTX1, and the similarity of the NMR chemicals shifts for the K–N rings (Table S2) provides further confirmation of the N-ring hemiketal in C-CTX1 and C-CTX5. The NMR data and periodate cleavage results are, therefore, consistent with the structure proposed by Lewis

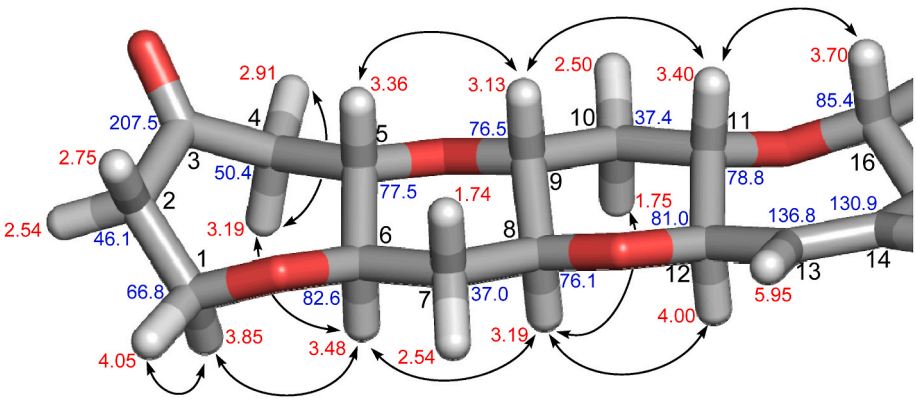

Fig. 5. Modelled 3-D structure of C-CTX5 showing the ring-A–D ring region of C-CTX5, with the ^{1}H (red) and ^{13}C (blue) chemical shift assignments (ppm) and their observed NOESY correlations.

Table 1
^{1}H and ^{13}C NMR assignments for C-CTX5 in C_5D_5N.[a]

Atom	^{13}C	^{1}H	Mult.	*J* (Hz)	Atom	^{13}C	^{1}H	Mult.	*J* (Hz)
1	66.8	3.85	dd	13.8, 11.5	33	83.8	3.34	~q	
		4.05	ddd	13.4, 5.0, 2.6	34	73.2	3.43	m	
2	46.1	2.54	m		35	46.7	1.50	m	
		2.75	ddd	18.0, 11.9, 5.1			1.81	~d	
3	207.5				36	28.1	1.86	m	
4	50.4	2.91	dd	13.2, 2.2	36-Me	28.4	0.91	d	7.2
		3.19	dd	13.2, 11.8	37	46.0	1.66	m	
5	77.5	3.36	ddd	11.7, 8.9, 2.7			1.97	~d	
6	82.6	3.48	ddd	11.2, 8.7, 4.3	38	81.4	3.14	~t	
7	37.0	1.73	~q		39	84.6	3.33	m	
		2.54	~d		40	37.0	1.72	~t	
8	76.1	3.19	m				2.54	~d	
9	76.5	3.13	~t		41	77.6	4.08	~t	
10	37.4	1.75	~q		42	79.7	3.54	td	9.0, 6.2
		2.50	~d		43	37.8	2.26	~d	
11	78.8	3.40	~t				2.70	m	
12	81.0	4.00	~d		44	74.7	4.12	m	
13	136.8	5.95	ddd	12.7, 4.8, 2.6	44-OH		6.26	br s	
14	130.9	5.81	dt	12.8, 2.5	45	79.9			
15	82.6	4.18	~d		45-Me	13.8	1.23	s	
16	85.4	3.70	~d		46	73.1	4.54	dd	13.0, 4.5
17	32.7	2.29	~d		47	44.1	2.13		
		2.84	~d				2.31		
18	125.8	5.84	m		48	78.7			
19	138.0	5.98	m	11.0, 5.9	48-Me	20.8	1.54	s	
20	84.0	4.13	~d		49	73.7	3.96	dd	–, 4.9
21	86.3	3.61	~d		50	25.5	1.76	~d	
22	33.1	2.27	m				1.94	m	
		3.03	m		51	25.2	1.90	~t	
23	128.4	6.00	br				2.02	m	
24	128.8	6.00	br		52	72.5	4.62	dd	11.6, 3.1
25	32.4	2.25	m		53	77.4			
		2.93	m		53-Me	18.9	1.46	s	
26	83.7	3.71	m		54	37.1	1.93	~d	
27	83.4	3.58	m				2.51	~t	
28	40.1	2.49	br m		55	29.8	2.04	~d	
		2.49	br m				2.14	~t	
29	74.8	4.10	m		56	96.3			
29-OH		5.15			56-OH		7.12		
30	78.6				57	69.6	3.96	s	
30-Me	9.9	1.26	s				3.96	s	
31	81.1	3.26	dd	12.1, 4.3	57-OH		6.57		
32	36.5	1.87	~q						
		2.25	~d						

[a] Mult. = ^{1}H multiplicity (s, singlet; d, doublet; t, triplet; quartet; br, broad, and; m, multiplet), with the associated coupling constants, where observed. Multiplicities preceded by ~ indicate apparent multiplicity in HSQC spectra, where only large couplings are observable. A detailed list of assignments and correlations is given in Table S1.

et al. [6] for C-CTX1, and with the structure established here for C-CTX5.

The NMR-based verification of the structure of C-CTX5, originally proposed by Mudge et al. [3] on the basis of chemical and biochemical transformations together with LC–HRMS/MS, highlights the power of that approach for identifying, with high certainty the structures of novel analogues when available in very limited amounts. With the

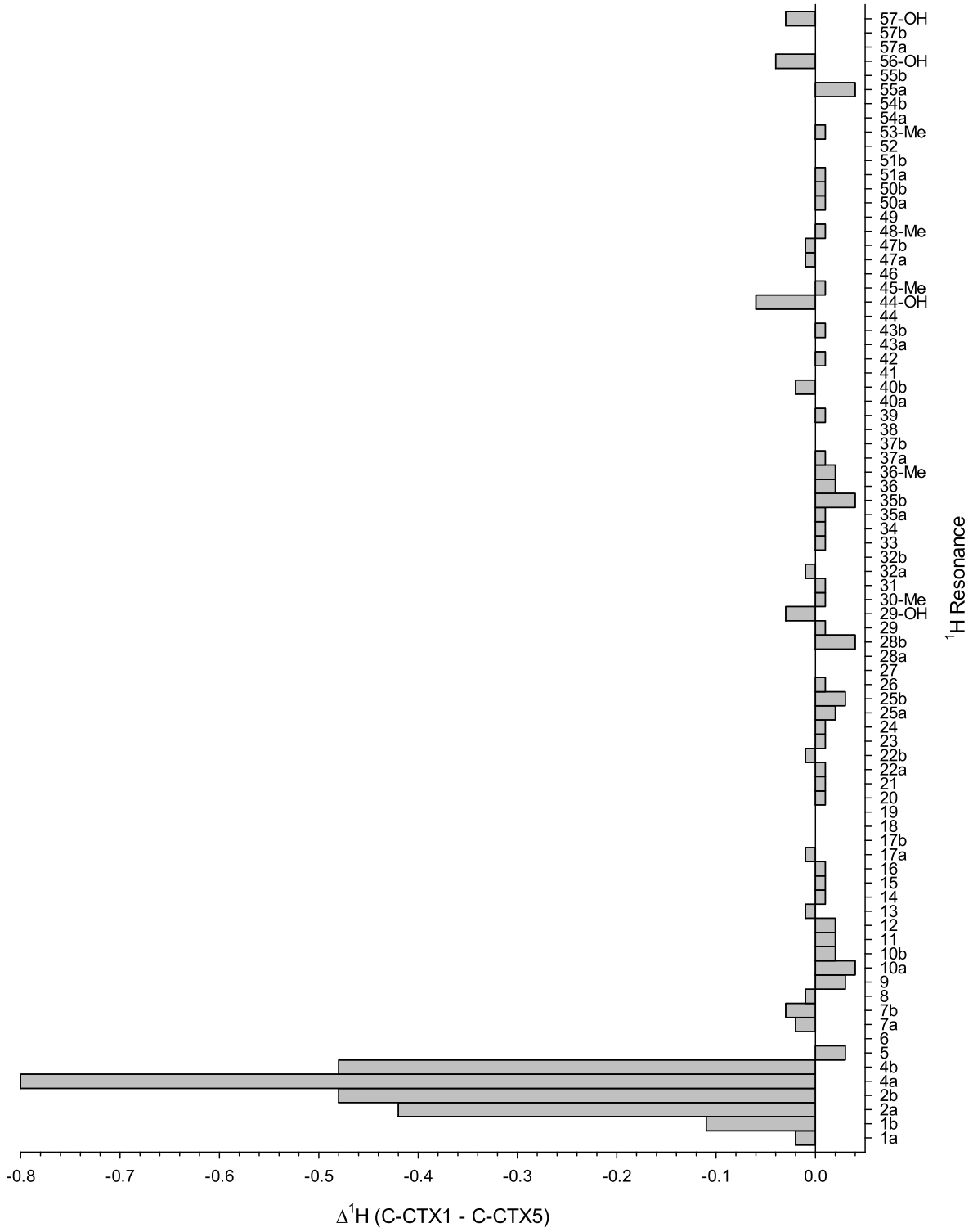

Fig. 6. ^{1}H chemical shift differences (ppm) between C-CTX1 [6] and C-CTX5 (Table 1), for each assigned resonance.

quantitation of the C-CTX5 by qNMR performed as part of the present study, we can now estimate that the C-CTX5 concentration was approximately 95 ng/mL in the original *G. silvae* 1602 SH-6 extract where C-CTX5 was discovered (based on peak area comparison of C-CTX5 in the extract to that of the quantified C-CTX5 solution), and that the fractions used by Mudge et al. [3] for its structure determination and microsome incubations contained in total approximately 100 ng of partially-purified C-CTX5. Judicious use of this strategy has the potential to provide structural information for compounds in mixtures where limited availability of sample, low concentrations of the analyte, or stability issues preclude traditional structure elucidation by purification and NMR spectroscopy.

The strategies employed here in the purification of C-CTX5 have potential application to the extraction and purification of other algal toxins, including other CTXs. For example, the present study utilised boric acid gel on a semipreparative scale for purification of C-CTX5, and Mudge et al. [12] have demonstrated that C-CTX1/2, C-CTX3/4, CTX1B, 54-deoxyCTX1B, and 52-*epi*-54-deoxyCTX1B also bind reversibly to

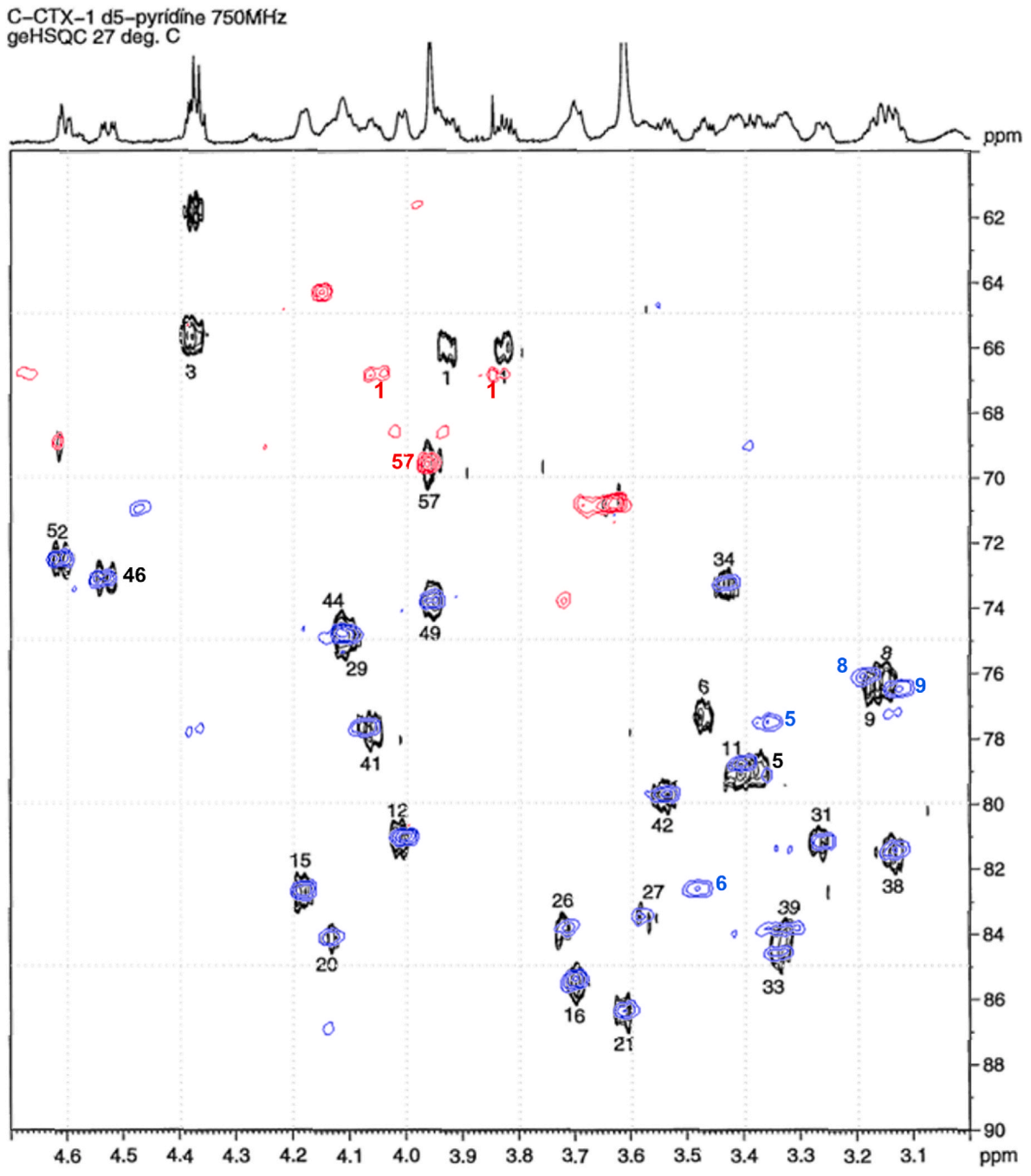

Fig. 7. Edited HSQC NMR spectrum of C-CTX5 (blue, CH; red, CH_2; 3.0–4.7 ppm) overlaid on the HSQC NMR spectrum of C-CTX1 (black) from the supporting information of Lewis et al. [6]. Black atom numbers are for C-CTX1 from Lewis et al., red and blue atom numbers are shown for correlations of C-CTX5 that differ significantly from those of C-CTX1. Both spectra were from d_5-pyridine calibrated to residual ^{1}H and ^{13}C solvent signals at 7.21 and 123.5 ppm. Adapted with permission from Lewis et al. [6]. Copyright 1998 American Chemical Society.

immobilized boronic acids, as do many gambierones, azaspiracids and tetrodotoxins [21–23]. This approach could be advantageous for extraction of CTXs from difficult matrices such as fish, where the analytes are usually present in very low concentrations, so that tedious multi-step cleanup procedures are often necessary before LC–MS analysis to reduce matrix effects and matrix interferences [24,25].

CRediT authorship contribution statement

Christopher O. Miles: Writing – review & editing, Writing – original draft, Visualization, Methodology, Investigation, Conceptualization. **Ian W. Burton:** Writing – review & editing, Writing – original draft, Visualization, Methodology, Investigation. **Nancy I. Lewis:** Writing – original draft, Investigation. **Alison Robertson:** Writing – review & editing, Resources, Funding acquisition. **Sabrina D. Giddings:** Writing – original draft, Investigation. **Pearse McCarron:** Writing – review & editing, Supervision. **Elizabeth M. Mudge:** Writing – review & editing, Writing – original draft, Visualization, Methodology, Investigation, Conceptualization.

Declaration of competing interest

The authors declare that they have no known competing financial interests or personal relationships that could have appeared to influence

the work reported in this paper.

Data availability

Data will be made available on request.

Acknowledgements

This research was funded by National Science Foundation (NSF) Partnerships in International Research and Education Program (Cigua-PIRE; 1743802 to AR) and the Research Council of Norway (Grant No. 279247 to Silvio Uhlig, Norwegian Veterinary Institute). This work also contributes to the National Institute of Environmental Health Science funded Greater Caribbean Center for Ciguatera Research (NIH: P01ES028949; NSF: 1841811 to AR). The authors thank Tyler B. Smith (University of the Virgin Islands) and Deana L. Erdner (University of Texas Marine Sciences Institute) and their lab personnel for the original collection of live algal material, isolation and culture establishment, and *G. silvae* identification.

Appendix A. Supplementary data

Supplementary data to this article can be found online at https://doi.org/10.1016/j.tet.2024.134115.

References

[1]. FAO and WHO, Report of the Expert Meeting on Ciguatera Poisoning, Food Safety and Quality Series, World Health Organization, Rome, 2020.
[2]. M.A. Friedman, L.E. Fleming, M. Fernandez, P. Bienfang, K. Schrank, R. Dickey, M.-Y. Bottein, L. Backer, R. Ayyar, R. Weisman, S. Watkins, R. Granade, A. Reich, Ciguatera fish poisoning: treatment, prevention and management, Mar. Drugs 6 (2008) 456–479.
[3]. E.M. Mudge, C.O. Miles, L. Ivanova, S. Uhlig, K.S. James, D.L. Erdner, C.K. Fæste, P. McCarron, A. Robertson, Algal ciguatoxin identified as source of ciguatera poisoning in the Caribbean, Chemosphere 138659 (2023).
[4]. M. Satake, Y. Ishibashi, A.-M. Legrand, T. Yasumoto, Isolation and structure of ciguatoxin-4A, a new ciguatoxin precursor, from cultures of dinoflagellate *Gambierdiscus toxicus* and parrotfish *Scarus gibbus*, Biosci. Biotechnol. Biochem. 60 (1996) 2103–2105.
[5]. M. Satake, M. Murata, T. Yasumoto, The structure of CTX3C, a ciguatoxin congener isolated from cultured *Gambierdiscus toxicus*, Tetrahedron Lett. 34 (1993) 1975–1978.
[6]. R.J. Lewis, J.-P. Vernoux, I.M. Brereton, Structure of Caribbean ciguatoxin isolated from *Caranx latus*, J. Am. Chem. Soc. 120 (1998) 5914–5920.
[7]. P. Estevez, M. Sibat, J.M. Leão-Martins, P. Reis Costa, A. Gago-Martínez, P. Hess, Liquid chromatography coupled to high-resolution mass spectrometry for the confirmation of Caribbean ciguatoxin-1 as the main toxin responsible for ciguatera poisoning caused by fish from European Atlantic coasts, Toxins 12 (2020) 267.
[8]. R.J. Clausing, H. Ben Gharbia, K. Sdiri, M. Sibat, M.L. Rañada-Mestizo, L. Lavenu, P. Hess, M. Chinain, M.-Y.D. Bottein, Tissue distribution and metabolization of ciguatoxins in an herbivorous fish following experimental dietary exposure to *Gambierdiscus polynesiensis*, Mar. Drugs 22 (2024) 14.
[9]. T. Ikehara, K. Kuniyoshi, N. Oshiro, T. Yasumoto, Biooxidation of ciguatoxins leads to species-specific toxin profiles, Toxins 9 (2017) 205.
[10]. F. Kryuchkov, A. Robertson, C.O. Miles, E.M. Mudge, S. Uhlig, LC–HRMS and chemical derivatization strategies for the structure elucidation of Caribbean ciguatoxins: identification of C-CTX-3 and -4, Mar. Drugs 18 (2020) 182.
[11]. R.R.L. Guillard, P.E. Hargraves, *Stichochrysis immobilis* is a diatom, not a chrysophyte, Phycologia 32 (1993) 234–236.
[12]. E.M. Mudge, A. Robertson, P. McCarron, C.O. Miles, Selective and efficient capture and release of *vic*-diol-containing Pacific and Caribbean ciguatoxins from fish extracts with a boronate affinity polymer, J. Agric. Food Chem. 70 (2022) 12946–12952.
[13]. I.W. Burton, M.A. Quilliam, J.A. Walter, Quantitative ^{1}H NMR with external standards: use in preparation of calibration solutions for algal toxins and other natural products, Anal. Chem. 77 (2005) 3123–3131.
[14]. J.-P. Vernoux, R.J. Lewis, Isolation and characterisation of Caribbean ciguatoxins from the horse-eye jack (*Caranx latus*), Toxicon 35 (1997) 889–900.
[15]. K. Yogi, N. Oshiro, Y. Inafuku, M. Hirama, T. Yasumoto, Detailed LC–MS/MS analysis of ciguatoxins revealing distinct regional and species characteristics in fish and causative alga from the Pacific, Anal. Chem. 83 (2011) 8886–8891.
[16]. F. Kryuchkov, A. Robertson, E.M. Mudge, C.O. Miles, S. Van Gothem, S. Uhlig, Reductive amination for LC–MS signal enhancement and confirmation of the presence of Caribbean ciguatoxin-1 in fish, Toxins 14 (2022) 399.
[17]. P. Estevez, J.M. Leao, T. Yasumoto, R.W. Dickey, A. Gago-Martinez, Caribbean ciguatoxin-1 stability under strongly acidic conditions: characterisation of a new C-CTX1 methoxy congener, Food Addit. Contam. 37 (2020) 519–529.
[18]. E.M. Mudge, A. Robertson, S. Uhlig, P. McCarron, C.O. Miles, 3-Epimers of Caribbean ciguatoxins in fish and algae, Toxicon 237 (2024) 107536.
[19]. P. Estevez, D. Castro, J. Manuel Leao, T. Yasumoto, R. Dickey, A. Gago-Martinez, Implementation of liquid chromatography tandem mass spectrometry for the analysis of ciguatera fish poisoning in contaminated fish samples from Atlantic coasts, Food Chem. 280 (2019) 8–14.
[20]. M. Sasaki, K. Iwasaki, K. Arai, Synthesis and structural implication of the JKLMN-ring fragment of Caribbean ciguatoxin C-CTX-1, J. Org. Chem. 86 (2021) 4580–4597.
[21]. D.G. Beach, E.S. Kerrin, P. McCarron, J. Kilcoyne, S.D. Giddings, T. Waaler, T. Rundberget, I.A. Samdal, K.E. Løvberg, C.O. Miles, Boronate techniques for clean-up and concentration of the *vic*-diol-containing tetrodotoxins and azaspiracids from shellfish, in: P. Hess (Ed.), Harmful Algae 2018 – from Ecosystems to Socioecosystems. Proceedings of the 18th Intl. Conf. On Harmful Algae. International Society for the Study of Harmful Algae, Nantes France, 2020, pp. 125–128.
[22]. C.O. Miles, J. Kilcoyne, P. McCarron, S.D. Giddings, T. Waaler, T. Rundberget, I. A. Samdal, K.E. Løvberg, Selective extraction and purification of azaspiracids from blue mussels (*Mytilus edulis*) using boric acid gel, J. Agric. Food Chem. 66 (2018) 2962–2969.
[23]. E.M. Mudge, A. Robertson, A.K. Leynse, P. McCarron, C.O. Miles, Selective extraction of gambierone and related metabolites in *Gambierdiscus silvae* using *m*-aminophenylboronic acid–agarose gel and liquid chromatography–high-resolution mass spectrometric detection, J. Chromatogr., B: Anal. Technol. Biomed. Life Sci. 1188 (2022) 123014.
[24]. R.J. Lewis, A. Yang, A. Jones, Rapid extraction combined with LC-tandem mass spectrometry (CREM-LC/MS/MS) for the determination of ciguatoxins in ciguateric fish flesh, Toxicon 54 (2009) 62–66.
[25]. J.S. Murray, M.J. Boundy, A.I. Selwood, D.T. Harwood, Development of an LC–MS/MS method to simultaneously monitor maitotoxins and selected ciguatoxins in algal cultures and P-CTX-1B in fish, Harmful Algae 80 (2018) 80–87.